AiMT Advances in Military Technology
Vol. 9, No. 2, December 2014

Technical Characteristics of Shells Conveyer

J. Balla and Z. Krist

University of Defence, Department of Weapons and Ammunition, Brno, Czech Republic

The manuscript was received on 30 September 2014 and was accepted after revision for publication on 29 November 2014.

Abstract:

The purpose of this article is to familiarize with new attitude to finding technical characteristics of the shells and charges conveyers used in heavy guns. The results are values of the hydraulic capacities, damping coefficient, and hydraulic resistances in the hydraulic circuits derived from own technical experiments. The kinematical parameters as are the conveyer velocity and conveyer acceleration are derived from the measured conveyer displacement. They enable with the measured input and output pressures, and the angular velocity of the hydraulic motor give expert opinion about conveyer operation as whole. The results are used for validation of the dynamic model, and they can be used as diagnostics data of the loading systems, and whole procedure as an example of the practicable technique in the higher military repair.

Keywords:

conveyer acceleration, conveyer velocity, conveyer displacement, damping coefficient, hydraulic capacity, hydraulic resistance, pressures in hydraulic motor, pressure derivative, Maltese cross

1. Introduction

The hydraulic drives of gun loading systems are used mainly for heavy tube weapons over 122 mm calibre using separated ammunition. The shell and the propellant charge are step by step loaded into the barrel, see [1]. Such a gun loading system represented in Fig. 1 consists of, see [2, 3]: shells storage system, case storage system, shells feeding device, case feeding device, ramming device, device for removing of cartridge cases from the loading system, and control system. The other parts in Fig. 1 serve to fulfil the whole functional cycle from one shot to another one. The shells storage system includes the box for shells, the conveyer of shells (it transports the shells to the feeding device), respectively the shells selection and the arrangement device (e.g. for the choice of the shell kind, the timing of the shell), see [4, 5]. The feeding device of shells transports the shells to the loading space. The charges storage system is similar to the shells storage system. The charges feeding device is similar to the shells feeding device, see [6]. The ramming device is arranged for different ramming displacement of shells and charges, [7, 8]. The device for removing cartridge cases from the loading system ensures the ejection of cartridge cases in the direction preventing any limitation of the next loading

cycle. The tasks of the control system are to open and to close the function of individual parts of the loading system and in some cases to control their velocities and accelerations.

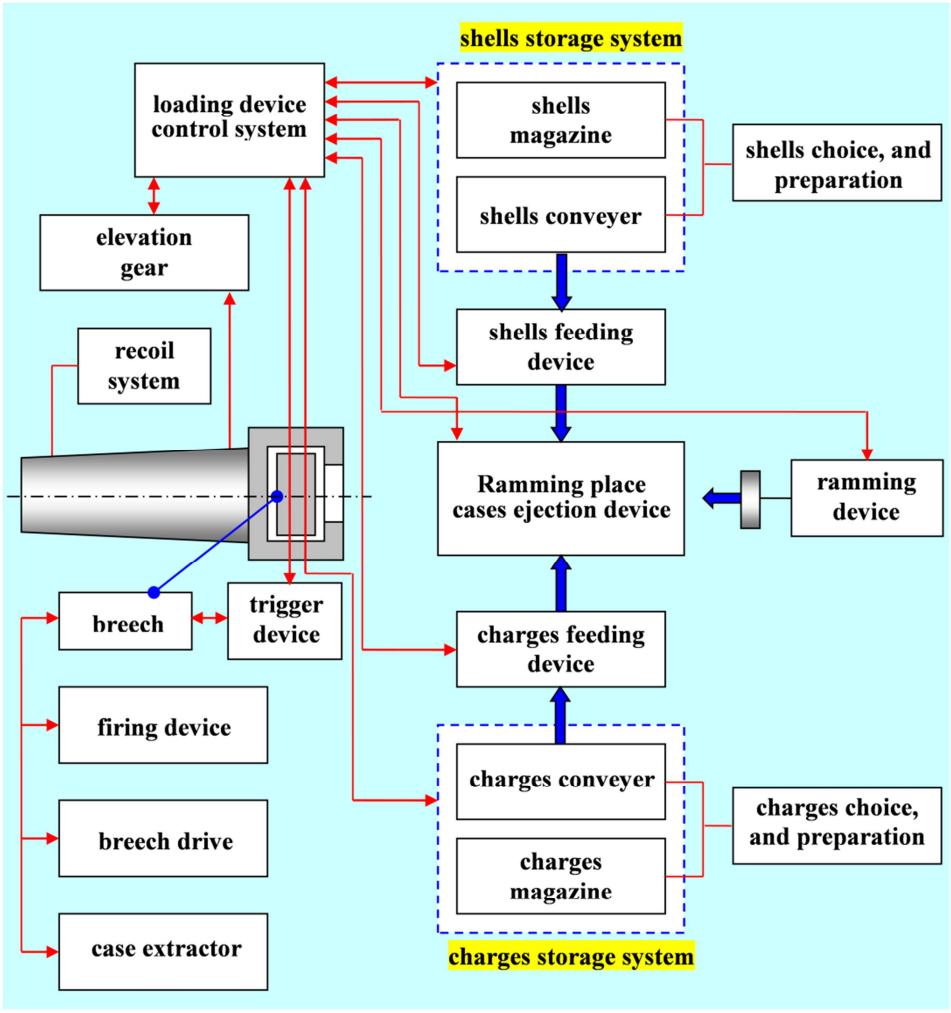

Fig. 1 Scheme of the loading system

The knowledge of the loading system main characteristics is necessary for the purposes of the design, system retrofitting, use, diagnostics and repairs. The performance of the loading system affects the reliability of the artillery gun when firing. The underestimation of the technical inspections and the loading system adjustment has recently resulted in several heavy gun breakdowns. Severe gun loading system damage can be avoided by careful monitoring of the loading system condition both before and after firing. Theoretical analyses and computer simulations performed at the University of Defence have revealed that no hydraulic characteristics can be set easily, mainly in repair units. The shells conveyer was the first part where measuring had been carried out on the loading system with the hydraulic drive. The essential results of the technical

experiments are presented in the next parts, and they enable to improve previous operational procedures in the armament service and to make the system calculations more accurate. The theoretical solution for the shells conveyer has been published in [2], and more general attitudes in modelling of systems are in [9].

2. Analytical Solution of Conveyer Movement

The 152mm self-propelled howitzer M77 has been used for technical experiments since it is frequently used in the Armed Forces of the Czech Republic and in other countries.

The shells and charges conveyers have the same mechanical system based on the Maltese cross ensuring the regular acceleration, breaking and stopping of the conveyer without impacts, see [5]. The kinematical scheme is represented in Fig. 2, see [2, 5]. An emergency drive by hand (with the angular velocity) is possible when the hydraulic drive does not operate due to the pump failure. The kinematical parameters as the displacement, velocity, and acceleration of the shells conveyer follow from the equation of the mechanical system motion, see [2, 7]

$$I_{\mathrm{M}}\ddot{\varphi}_1 + 0.5\omega_1^2 \frac{\mathrm{d}I_{\mathrm{M}}}{\mathrm{d}\varphi_1} = M_{\mathrm{M}} - M_{\mathrm{Z}} - M_{\mathrm{D}}, \tag{1}$$

where

I_{M} – the reduced mass moment of inertia of the whole system (kg m^2),

φ_1 – the angular displacement of the hydraulic motor shaft (rad),

ω_1 – the angular velocity of the hydraulic motor shaft (rad s^{-1}),

$\ddot{\varphi}_1$ – the angular acceleration of the hydraulic motor shaft (rad s^{-2}),

M_{M} – the hydraulic motor driving torque (N m),

M_{Z} – the reduced moment of workload (N m),

M_{D} – the damping moment of the hydraulic motor (N m).

The M_{M} driving torque depends on the p_1 input pressure and p_2 output pressure according to the formula

$$M_{\mathrm{M}} = \frac{V_{\mathrm{G}}}{2\pi}(p_1 - p_2), \tag{2}$$

where

V_{G} – the geometrical volume of the hydraulic motor.

The pressures p_1 and p_2 are derived from the scheme of the hydraulic circuit in Fig. 3 and from the following differential equations of the first order with hydraulic losses denoted by Z_1, Z_2:

$$\frac{\mathrm{d}p_1}{\mathrm{d}t} = \frac{\left(Q_1 - \frac{V_G}{2\pi}\omega_1 - Z_1 p_1\right)}{C_1}, \tag{3}$$

and

$$\frac{\mathrm{d}p_2}{\mathrm{d}t} = \frac{\left(\frac{V_G}{2\pi}\omega_1 - Q_2 - Z_2 p_2\right)}{C_2}, \tag{4}$$

where

Q_1 – the input flow of hydraulic motor ($m^3\ s^{-1}$),

Q_2 – the output flow of hydraulic motor ($m^3\ s^{-1}$),

Z_1 – the input hydraulic losses ($m^3\ s^{-1}\ Pa^{-1}$),

Z_2 – the output hydraulic losses ($m^3\ s^{-1}\ Pa^{-1}$).

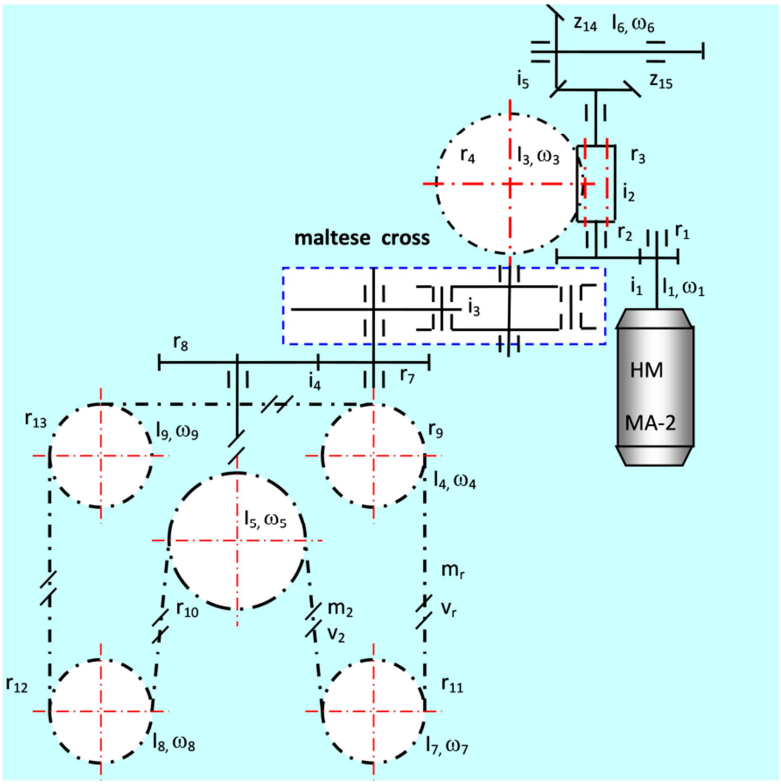

Fig. 2 Kinematic scheme of the shell conveyer

The input and output hydraulic capacities C_1 and C_2 are given, see [2, 4]:

$$C_1 = \beta_L V_{01}, \tag{5}$$

and

$$C_2 = \beta_L V_{02}, \tag{6}$$

where

V_{01} – the input liquid volume in the pipe, leading from distributor to hydraulic motor (m^3),

V_{02} – the output liquid volume in the pipe, leading from hydraulic motor to distributor (m^3),

β_L – the liquid volume compressibility factor, there $\beta_L = 6.8 \times 10^{-10}$ Pa^{-1}, see [8].

The compressibility factor β_L has to be considered as a reduced parameter including the liquid elastic properties, tubes, and the air bubbles presented in the liquid. Their exact finding is theoretically difficult and the experimental methods seem to be more appropriate, see [2].

3. Technical Experiments on Shells Conveyer

The shaft having the ω_6 angular velocity, see Fig. 2, has been chosen as the part connecting the drive with the speed voltage generator measuring angular velocity of the hydraulic motor. The linear conveyer displacement x_{CONV} having the own mass m_r (Fig. 2) is the second kinematical parameter. Finally the hydraulic characteristics (the generator pressure p_G, the input pressure p_1, the output pressure p_2, and the waste pressure p_3) are marked in Fig. 3 which shows the simplified hydraulic circuit of the shells conveyer drive.

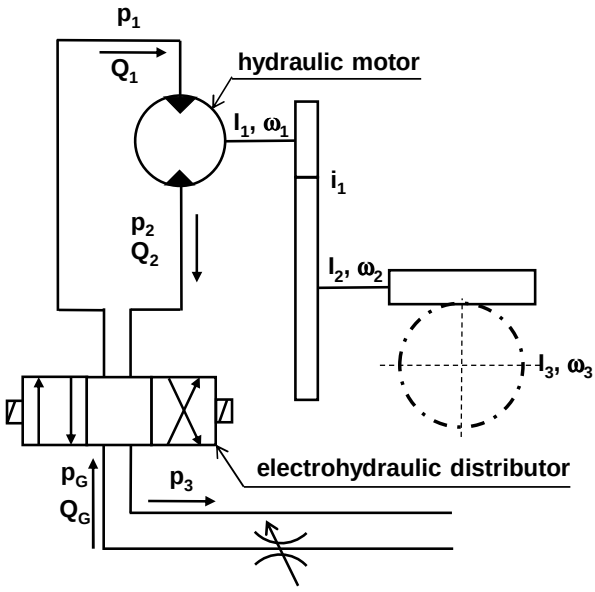

Fig. 3 Scheme of the shells conveyer hydraulic circuit

The output shaft angular velocity ω_1 of the hydraulic motor has been determined using of the K4A2 speed voltage generator from the kinematic ratio between both angular velocities it follows:

$$\frac{\omega_1}{\omega_6} = 3.$$

The strain gauge pressure sensors located in the required places on the shell conveyer have ranges up to 40 MPa, which is sufficient for this purpose. The electrohydraulic distributor enables to drive conveyer on both sides according to the required loading program, regularly according to the control system, and backwards in case of the shells conveyer loading or unloading. The throttle valve ensures the setting of the hydraulic motor shaft rotation. The WL250 inductive displacement sensor, measuring the conveyer displacement x_{CONV} with the range of 250 mm, is connected with the moving part of the conveyer, and it had to be manually returned into the initial position after every measuring cycle. The five measured signals, i.e. p_{G}, p_1, p_3, ω_1, and x_{CONV}, had been stored in the MC-32 measuring system and afterwards have been analysed using the Next View® software, see [10]. The 500 Hz sampling frequency had been sufficient for this purpose. The formerly made external amplifiers (Microtechna M1000) had been set up to the 100 Hz cut-off frequency by means of the 8$^{\mathrm{th}}$ order Butterworth low-frequency filter. After Next View® software analysis the results had been exported in Microsoft Excel® format or in ASCII format. Finally the results have been drawn in MATLAB® software. The other possibilities of analyses of the measured data are published in [11, 12].

In course of results analysis, the conveyer displacement record has been reduced with the reduction rate 1:10. The procedure is known as the data decimation when the sampling frequency is reduced by an integer factor, see [10]. This reduction proved to be better due to the following differentiation instead of the signal filtering when the phase shift comes up among the courses of the conveyer displacement, the conveyer velocity and the conveyer acceleration. Moreover the very low frequency range of the conveyer movement enables to reduce number of measured data, see [10-12].

The results of the kinematic values when conveyer is empty are displayed in Fig. 4, where x_{CONV}, v_{CONV}, a_{CONV} are the conveyer displacement, conveyer velocity, and conveyer acceleration. The two last values have been set after differentiation of the x_{CONV}. The shell conveyer displacement is conducted in two stages and its velocity rises from zero value to the maximal one of 0.24 $\mathrm{m\,s^{-1}}$ after the drive acceleration. According to the Directive for maintenance the conveyer cycle time has to be in the range from 2.5 s to 3 s, see [13, 14].

These kinematic characteristics have been chosen for validation of the mathematical model of the shell conveyer published in [5]. The kinematic parameters correspond to the calculations. The overall conveyer stroke is 203 mm during two stages according to the Maltese cross design. The idle periods at the beginning, at the middle, and at the end of operation are necessary to prevent an impact action. The observed pressures are drawn in Fig. 5. The source pressure p_{G} steadily drops during conveyer operation. The input pressure p_1 varies according to the conveyer workload and the waste pressure p_3 has approximately the same value during the operational stage of the conveyer. The small "noise" in the p_1, p_3, and p_{G} signals is probably caused with the operation of the hydraulic source having the axial hydraulic pump with the control overflow valve. The other presumptive cause of the noise is the vibration of the electrohydraulic distributor piston during changes of the mass moment of inertia system and the system workload. The spectral tests proved that the frequencies presented in hydraulic circuits are less than 100 Hz as it was expected, and it was the reason why these filters have been used.

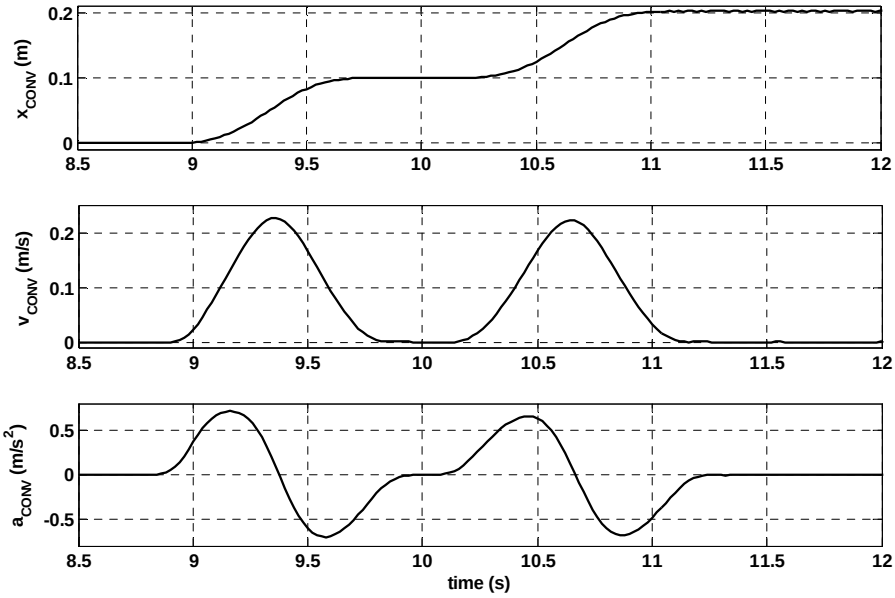

Fig. 4 Kinematic characteristics of shells conveyer

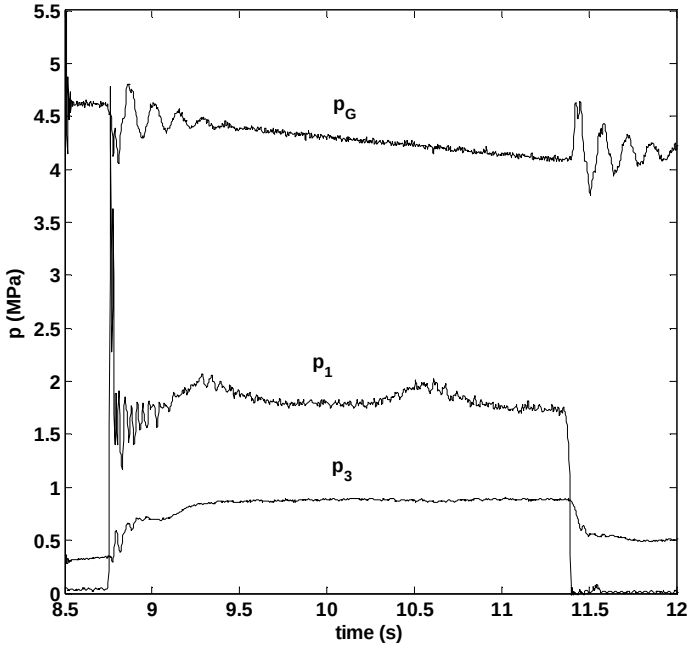

Fig. 5 Pressures in conveyer hydraulic circuits

By using these results and the angular velocity of the hydraulic motor shaft ω_1, see Fig. 6, the following values have been determined: the damping coefficient of the

hydraulic motor b_D used in Eq. (1) as a part of the damping moment M_D, and the hydraulic capacities of the system C_1, C_2 in Eq. (5), Eq. (6). After comparing the p_1 measuring with the calculation of $\frac{dp_1}{dt}$ and $\frac{dp_2}{dt}$, the hydraulic capacities have been set as follows: $C_1 = 8 \times 10^{-12}$ m^3 Pa^{-1}, and $C_2 = 6 \times 10^{-12}$ m^3 Pa^{-1}. The capacities influence the initial rise of the pressure after starting.

The example of the $\frac{dp_1}{dt}$ time-history diagram compared with the p_1 in Fig. 7 enabled to set the hydraulic capacity in the hydraulic motor circuit. Only at the beginning and at the end of the operation of the electrohydraulic distributor, $\frac{dp_1}{dt}$ varies, and during the steady state the member $\frac{dp_1}{dt} \to 0$. It means that the change of the hydraulic capacity can be neglected during conveyer drive since in case of the $\frac{dp_1}{dt}$ change only the hydraulic motor and one part of the gearbox is moving. The utilization of the course of the angular velocity in Fig. 6 enables to set the required input flow of the hydraulic motor.

According to the known simple formula, the minimal input flow in the operation stable state without losses after neglecting of the hydraulic capacities is

$$Q_1 = \frac{V_G}{2\pi}\omega_1, \tag{7}$$

and it achieves about 0.5×10^{-6} m^3 s^{-1}.

The estimation of the hydraulic resistances for input and output circuits can be set using of the stable state equation, see [4] and [5]

$$Q_1 = \operatorname{sgn}\left(p_G - p_1\right)\sqrt{\frac{\left|p_G - p_1\right|}{R_1}}, \tag{8}$$

and

$$Q_2 = \operatorname{sgn}\left(p_2 - p_0\right)\sqrt{\frac{\left|p_2 - p_0\right|}{R_2}}. \tag{9}$$

After rearrangements and excluding the resistances R_1, and R_2 from (8), and (9) we get the hydraulic resistances of the input and output parts as follows:
$R_1 = 7.1 \times 10^{12}$ Pa s^2 m^{-6}, $R_2 = 2.45 \times 10^{12}$ Pa s^2 m^{-6}.

The motor operation starts at time t = 8.75 s and ends at t = 11.4 s as measured. The time was measured from the beginning until the closing of the electrohydraulic distributor. Then, the operation time of empty conveyer is 2.65 s.

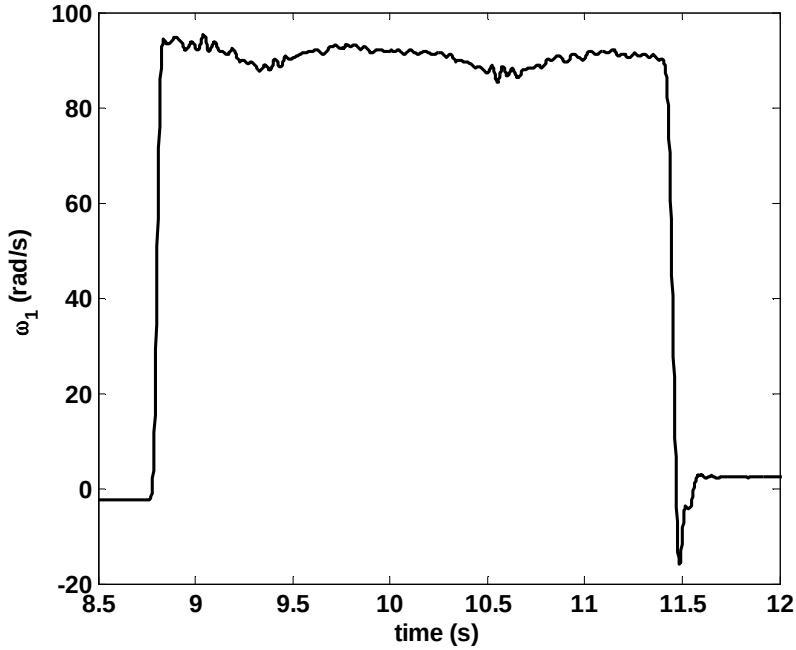

Fig. 6 Hydraulic motor shaft angular velocity

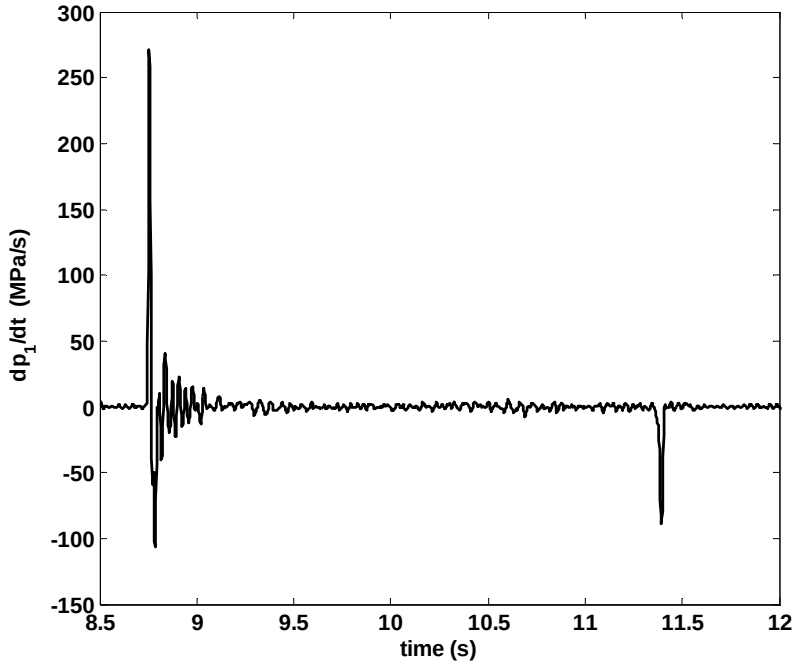

Fig. 7 Input pressure derivative/time history

The damping moment given in the motion equation (1) depends on the input angular velocity of the hydraulic motor shaft according to formula

$$M_{\mathrm{D}} = b_{\mathrm{D}}\omega_1, \tag{10}$$

where the mean value of the damping coefficient $b_{\mathrm{D}} = 0.036$ N m s rad^{-1} has been determined by the measurement in the course of steady-state motion of the system under off-load conditions. The input pressure p_1 and the angular velocity ω_1 in Fig. 5 and Fig. 6 have been used for that purpose.

In case of conveyer workload, the operation time is somewhat longer, about 80 ms, as it is depicted in Fig. 8 and Fig. 9. The time was set by a similar way as before. One phenomenon is representative of these mechanisms, as introduced in [2, 5, 7]. In contradiction to classical mechanism having constant transmission ratio, this one operated using the Maltese cross; the time of conveyer velocity drop is shorter than when the conveyer is empty. It is given by the second member on the left side in Eq. (1) causing the return of the kinetic energy of the mechanical system during the conveyer velocity drop. The maximal value of workload (when conveyer is full, having 36 shells and its mass is approximately 1790 kg) is several times greater than without shells (200 kg. It produces the great changes of the inertia mass moment I_{M} and the reduced moment of workload M_{Z} in Eq. (1). The time differences between the v_{CONV} conveyer velocity rise and the v_{CONV} conveyer velocity drop are several milliseconds in case of the empty conveyer, and several tens milliseconds when the conveyer is full.

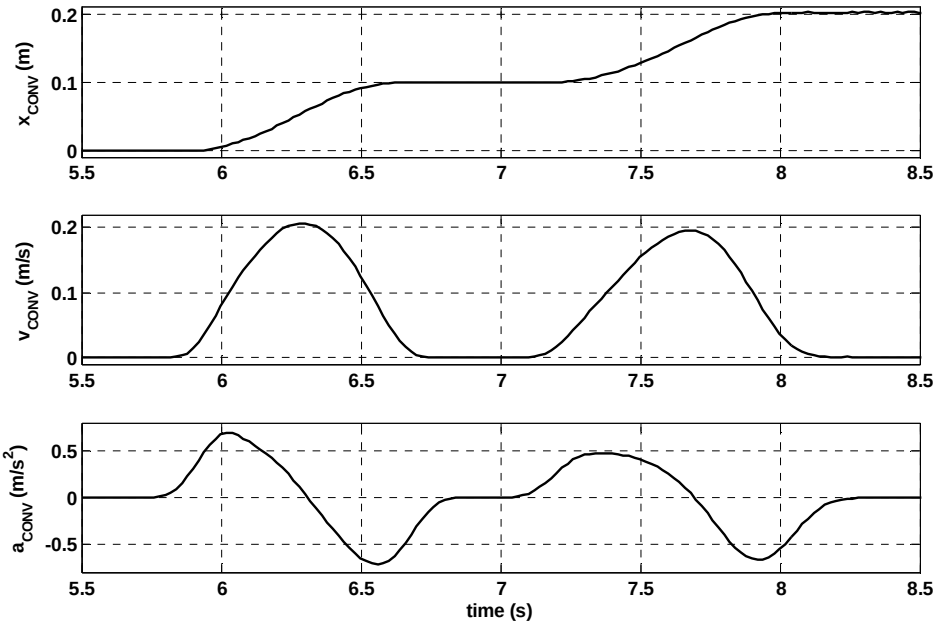

Fig. 8 Kinematic characteristics – conveyer is under workload

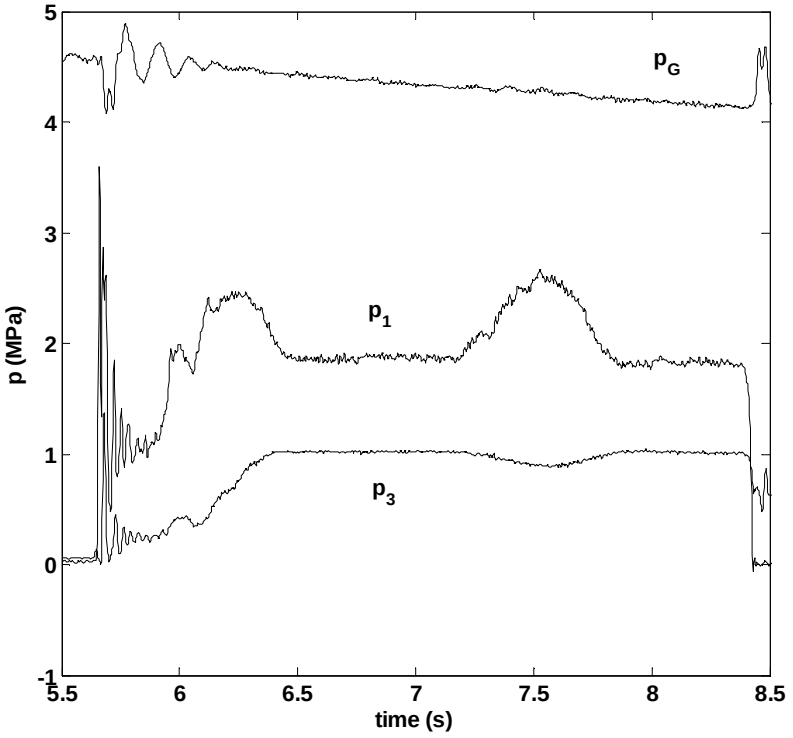

Fig. 9 Pressures – conveyer is under workload

4. Conclusions

The article describes the original methods of kinematical and hydraulic parameters setting that have been used for validation of the calculations and diagnostic signals in the service. The asset of here published methods is that they enable to determine the technical parameters of the conveyers which are not easily detectable, and they extend the diagnostic possibilities to the other weapon systems with the hydraulic drives, see [13, 14]. Finally the course in Figs 4 to 9 has been compared with calculations in [2, 5] with errors under 10 %. The method of setting the kinematic and hydraulic parameters can be used for diagnostic purposes where not only the time of operation can be determined, as it was before. The diagnostic signals described here – conveyer displacement, input pressure, angular velocity, and their mathematical derivatives – proved to be convenient. The methods are suitable for using in current loading systems with hydraulic drives.

The main kinematical and hydraulic parameters used in Eqs (1), (3), and (4), and proposed for the conveyer diagnostics purposes are given in Tab. 1. From Tab. 1 it is clear that the system of the conveyer drive has the sufficient power reserve since it is able to work without any sophisticated control system both with and without higher workload. The differences are only several milliseconds in cycle time, and a few hundredths of a m/s in the conveyer velocity. On the other hand, these values depend on the pressure course versus time of the hydraulic generator. It has to be taken into

consideration when the system is driven with an emergency source of the hydraulic energy, and in course of malfunctions.

Tab. 1 Parameters set by measuring

Symbol	Quantity	Value
t_{Cempty}	empty conveyer cycle time	2.65 s
t_{Cfull}	full conveyer cycle time	2.73 s
v_{CONV}	maximal empty conveyer velocity	0.2 m/s
v_{CONV}	maximal full conveyer velocity	0.23 m/s
b_{D}	damping coefficient of system	0.036 N m s rad^{-1}
C_1	input hydraulic capacity	8×10^{-12} m^3 Pa^{-1}
C_2	output hydraulic capacity	6×10^{-12} m^3 Pa^{-1}
R_1	input hydraulic resistance	7.1×10^{12} Pa s^2 m^{-6}
R_2	output hydraulic resistance	2.45×10^{12} Pa s^2 m^{-6}

In future there are several possibilities for using of an offline identification method as it is mentioned in [12], searching the other parameters, such as transfer function and losses in the hydraulic circuits at the beginning of the conveyer operation.

Acknowledgement

This work was supported by the research project: Research project of Weapons and ammunition department 2014, No. 907930101023, University of Defence.

References

[1] MACKO, M. and BRABCOVA, K. Assessment of the use of smart artillery ammunition in future military operations. In *The 18th International Conference Knowledge-Based Organization. Conference Proceedings 1. Management and Military Sciences*. Sibiu: Nicolae Balcescu Land Forces Academy, 2012, p. 28-32.

[2] BALLA, J., DUONG, VY. and KRIST, Z. Dynamics of shell conveyer with Maltese cross. *International Journal of Mechanics*, 2013, vol. 7, no. 2, pp. 81-89.

[3] BALLA, J., MACKO, M. and POPELINSKY, L. *Guns II*. Brno: University of Defence, 2010, 72 p.

[4] BALLA, J. Twin motor drives in weapon systems. *WSEAS Transactions on Systems and Control*, 2010, vol. 5, no. 9, p. 755-765.

[5] BALLA, J. and DUONG, VY. Maltese Cross in One Weapon Application. In *Proceedings of the 14th WSEAS International Conference on Mathematical and Computational Methods in Science and Engineering (MACMESE '12)*. Sliema: WSEAS Press, 2012, p. 182-187. ISBN 978-1-61804-117-3.

[6] BALLA, J. and DUONG, VY. Analysis of feeding device with two degrees of freedom. *International Journal of Mechanics*, 2011, vol. 5, no. 1, p. 361-370. ISSN 1998-4448.

[7] BALLA, J. and KRIST, Z. Determination of shells conveyer parameters. In *Proceedings of the 10th International Conference on Applied and Theoretical Mechanics (MECHANICS'14)*. Salerno: WSEAS Press, 2014, p. 181-187. ISSN 2227-4588.¨

[8] BALLA, J. Kinematics and dynamics of ramming devices. *Advances in Military Technology*, 2008, vol. 3, no. 1, p. 93-104. ISSN 1802-2308.

[9] BALLA, J., PROCHAZKA, S. and DUONG, VY. Evaluation of projectile ramming process in new and worn smooth barrels of guns. *International Journal of Mechanics*, 2013, vol. 7, no. 2, p. 136-144. ISSN 1998-4448.

[10] *Next View 4.3 professional software documentation*. Maisach: BMC Messsysteme GmbH, 2009.

[11] VITEK, R. Measurement of the stereoscopic rangefinder beam angular velocity using the digital image processing method. In *Proceedings of the 12th WSEAS International Conference on Mathematical and Computational Methods in Science and Engineering*. Faro: WSEAS Press, 2010, p. 230-235. ISBN 978-960-474-243-1.

[12] DUB, M. and JALOVECKY, R. DC Motor Experimental Parameter Identification using the Nelder-Mead Simplex Method. In *Proceedings of 14th International Power Electronics and Motion Control Conference (EPE/PEMC 2010)*, p. S4-9 to S4-11. ISBN 978-1-4244-7856-9.

[13] Military Directive Děl-22-40/4. *152mm SPH M77 Technical inspections and maintenance I* (in Czech). Prague: Ministry of Defence, 1987.

[14] Military Directive Děl-22-40/5. *152mm SPH M77 Technical inspections and maintenance II* (in Czech). Prague: Ministry of Defence, 1989.